Journal of
Water & Climate Change

IWA PUBLISHING

Journal of Water and Climate Change Vol 15 No 3, 1142 doi: 10.2166/wcc.2024.499

Evaluation of evapotranspiration using energy-based and water balance hydrological models

Ressy Fitria [a,*], Michael Timothy[b] and Roald Marck J. Revellame[c]

[a] Department Geodetic Engineering, Faculty of Engineering, Universitas Gadjah Mada, Yogyakarta, Indonesia
[b] Surveyor Indonesia, Jakarta, Indonesia
[c] National Irrigation Administration, Metro Manila, Philippines
*Corresponding author. E-mail: ressyfitria@ugm.ac.id

RF, 0000-0003-4056-7522

ABSTRACT

The reliability of evapotranspiration (ET) models is crucial to comprehending land–atmosphere interactions and water balance dynamics in various available resources of the model. This study compared two different models based on energy and water balance models, a surface energy balance system (SEBS) and spatial processes in hydrology (SPHY), evaluated against ground observation data from flux towers for different land-cover characteristics (forest and savanna) in southeast Africa. We found that both models have good correlation with flux-tower data for both sites (ZM-Mon and ZM-Kru). The SEBS model showed a lower root-mean-square error (RMSE; 2.17 mm day^{-1}) at the savanna site (ZM-Kru) than the SPHY model (2.27 mm day^{-1}). However, at the forest site (ZM-Mon), the SEBS model showed a higher RMSE value (1.90 mm day^{-1}) than the SPHY model (0.88 mm day^{-1}). Then, we analyzed the ET model's sensitivity to the precipitation variable. We found that SPHY overestimated ET during the winter season and underestimated it during the summer season, which might be influenced by the dependency of the SPHY model on water excess and water shortage stress parameters in ET calculations. Overall, SPHY, with fewer input data, showed a reasonably good result compared with SEBS. The results revealed that each model possesses its unique strengths and limitations in relation to specific land covers and vegetation composition, offering opportunities for improvement and optimization.

Key words: energy-based, evapotranspiration, land cover, SEBS, SPHY, water balance

HIGHLIGHTS

- The water balance model with fewer input data showed a reasonably good result compared with the energy-based model.
- The SEBS model showed a lower RMSE at the savanna site and a higher RMSE at the forest site than the SPHY model.
- SPHY overestimated ET during the winter season and underestimated it during the summer season.

GRAPHICAL ABSTRACT

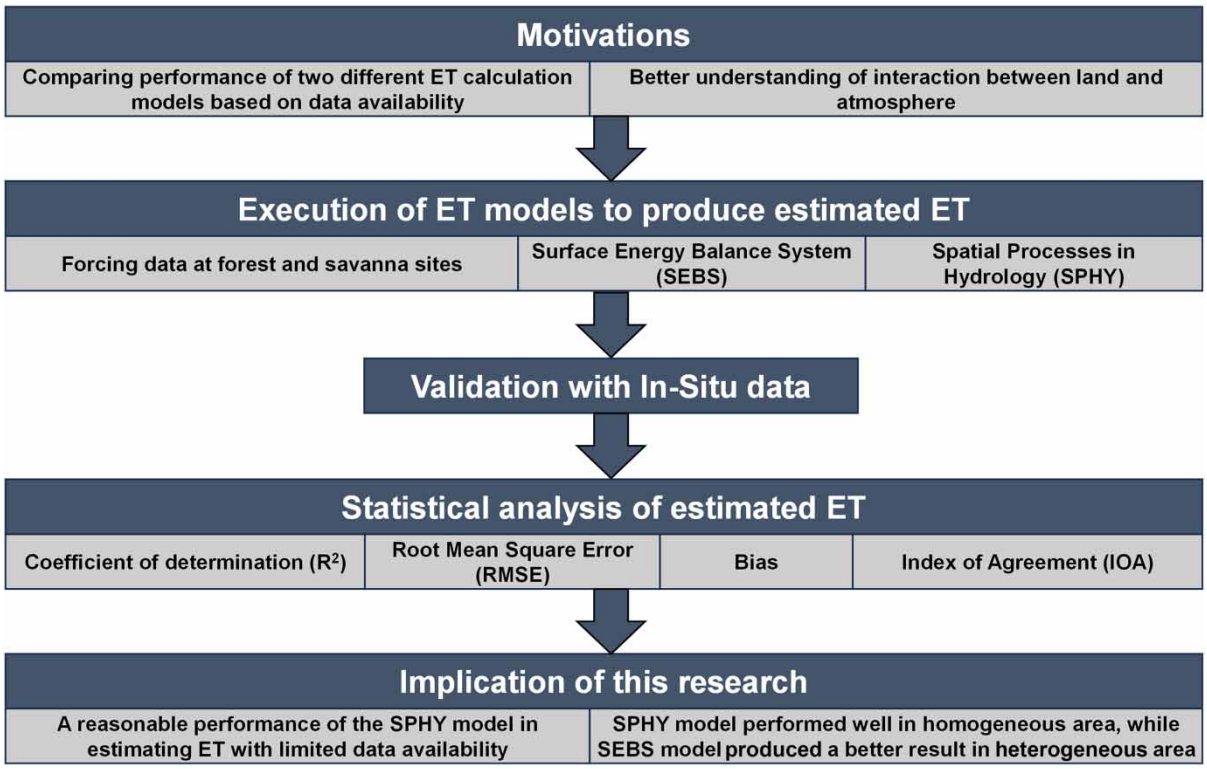

1. INTRODUCTION

Evapotranspiration (ET) is the process by which water is transferred from the Earth's surface to the atmosphere and is a critical component of the Earth's water cycle to understand the link between land surface and atmosphere (Brutsaert 1982). It depends on both biophysical and environmental processes involved in the interaction between soil, vegetation, and atmosphere (Allen *et al.* 1998; Fisher *et al.* 2008; Ershadi *et al.* 2014). Therefore, considering ET has a major role in regulating climate and hydrology, it should be accurately quantified for proper decision-making in water resource management (Senay *et al.* 2011; Hwang & Choi 2013; Liaqat & Choi 2015).

The limited networks of ET monitoring stations pose challenges in providing global or regional quantification of ET (Long *et al.* 2014). Remotely sensed data provide an opportunity to estimate spatial and temporal variations of ET. One of the developed models that used satellite remote sensing is the surface energy balance system (SEBS). The SEBS model was developed by Su (2002) based on the energy balance equation. The SEBS is a widely validated model to calculate the turbulent heat fluxes for the hydrological model from the point scale to the regional scale and requires a high amount of data as inputs (Chen *et al.* 2013; Lu *et al.* 2013). The SEBS has been useful in estimating the actual ET in different river basins (Liaqat & Choi 2015; Liaqat *et al.* 2015) and different types of biomes, such as grassland, cropland, and evergreen needleleaf forest (Gokmen *et al.* 2012; Ma *et al.* 2012; Byun *et al.* 2014; Ershadi *et al.* 2014).

Another method to calculate ET is using hydrological models. In recent years, there has been a growing interest in using hydrological models to simulate ET. Hydrological models can be used to estimate ET at various scales, from local to regional to global, including different temporal scales. One of the newly developed hydrological models is spatial processes in hydrology (SPHY), introduced by FutureWater (Terink *et al.* 2015b; Eekhout *et al.* 2018). The SPHY model links the element of water balance components and simplifies the real-world complexity, requiring only temperature and precipitation as the main dynamical input data.

To address the tradeoff between data requirements and performance outcomes, this research compares and contrasts two models: one model has comprehensive data requirements, known for providing detailed energy-balance component results,

while the other model estimates acceptable water balance component results with fewer inputs. This paper evaluates the performance of two energy-based and water balance hydrological models in simulating ET over southeast Africa. The two models are the surface energy balance system (SEBS) and the spatial processes in hydrology (SPHY) model, representing the energy-based and water balance-based hydrological models, respectively. In this study, we compare ET products from different model frameworks to evaluate the performance of models at different land covers. We also analyzed the relationship between hydrological variables and the ET output of the hydrological model. This work is expected to benefit future studies on machine-learning paradigms in terms of selecting data usage for ET prediction by examining the correlation between the amount of input data and model efficiency.

2. STUDY AREAS AND METHODS

2.1. Study area

Southeast Africa was selected to evaluate ET products from both models (Figure 1). In this area, two sites with land cover of deciduous broadleaf forests (ZM-Mon) and savannas (ZA-Kru) were selected because of the availability of ground observation data to analyze the ET in different ecosystems with various plant functional types (PFTs), soil properties, and climate variables. The mean annual temperature and precipitation are listed in Table 1 for all sites, along with their location and hydro-meteorological characteristics. We selected a study period spanning two years (2008–2009).

The Skukuza site is characterized by a subtropical arid steppe hot climate type based on the Köppen–Geiger climate classification, while the Mongu site experiences a tropical wet and dry climate. Both Skukuza and Mongu sites have the highest rainfall in the summer season, occurring from December to February (wet period), while the driest season occurs from June to August, with little to no rainfall (Queface *et al.* 2011).

2.2. SEBS model

2.2.1. Methods

The SEBS model was developed based on the energy balance equation to estimate actual ET in situations where water is limited. The effectiveness of the SEBS model has been evaluated in a variety of habitats and climatic settings (Su 2002). The energy balance can be represented as follows:

$$R_N = G + H + \mathrm{LE} \tag{1}$$

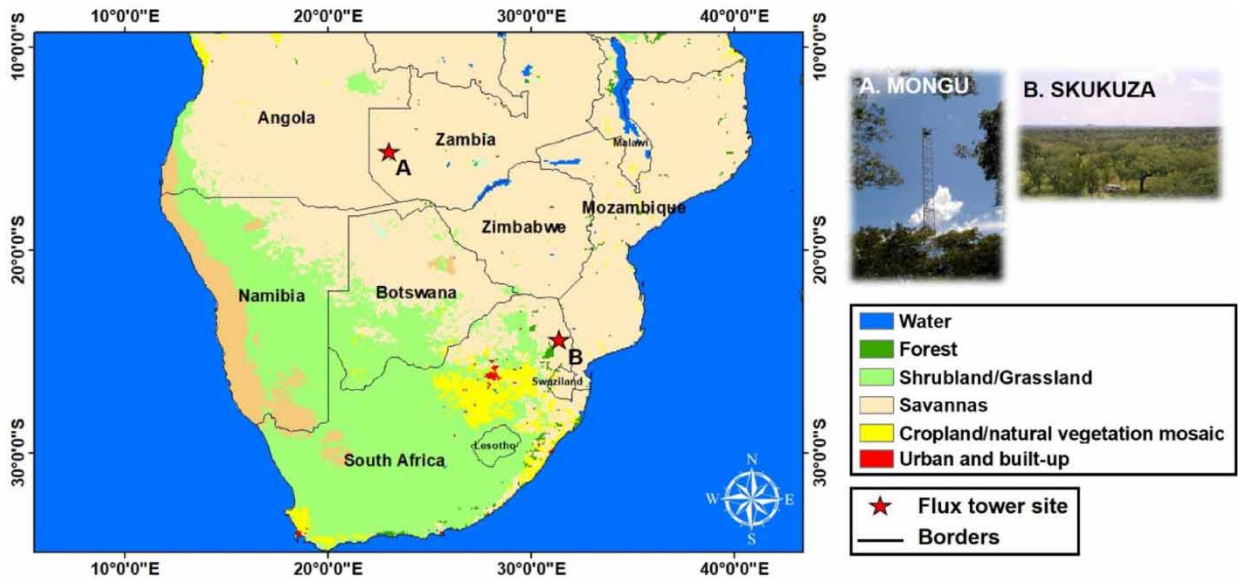

Figure 1 | Study sites in southeast Africa with different land-cover types.

Table 1 | Characteristics of selected study sites

Site	Location			Plant functional type	Mean annual temperature (°C)	Mean annual precipitation (mm)
	Latitude	Longitude	Elevation (m)			
Mongu (ZM-Mon)	−15.4378	23.2528	1,053	Deciduous broadleaf forest (DBF)	25	945
Skukuza (ZA-Kru)	−25.0197	31.4969	359	Savannas (SAV)	21.9	547

where R_N is the net radiation (W m^{-2}), LE is the latent heat flux (W m^{-2}), H is the sensible heat flux (W m^{-2}), and G is the heat flux through the soil (W m^{-2}). The Monin–Obukhov similarity theory was used to evaluate the sensible and latent heat flux. The atmospheric surface layer (ASL) and the atmospheric boundary layer are distinguished in the SEBS. The profiles of the mean wind speed (u) and the mean temperature (θ_0–θ_a) are similar in terms of their expressions in the ASL and are expressed as follows (Su 2002):

$$u = \frac{u_*}{k}\left[\ln\left(\frac{z-d_0}{z_{0m}}\right) - \Psi_m\left(\frac{z-d_0}{L}\right) + \Psi_m\left(\frac{z_{0m}}{L}\right)\right] \tag{2}$$

$$\theta_0 - \theta_a = \frac{H}{ku_*\rho C_p}\left[\ln\left(\frac{z-d_0}{z_{0h}}\right) - \Psi_h\left(\frac{z-d_0}{L}\right) + \Psi_h\left(\frac{z_{0h}}{L}\right)\right] \tag{3}$$

where u_* represents the friction velocity (m s^{-1}), z is the height of measurement, z_{0m} is the roughness length for momentum transfer (m), z_{0h} is the roughness length for heat transfer (m), d is the zero-displacement height (m), k is the von Karman's constant, θ_0 is the potential temperature on the surface (K), θ_a is the potential air temperature at z (K), C_p is the specific heat capacity of air at constant pressure (J kg^{-1} K^{-1}), Ψ_m and Ψ_h are the stability correction functions for momentum and heat transfer, respectively, and L is the Obukhov length (m).

The zero-displacement height (d) and the roughness length (z_{0m} and z_{0h}) play a vital role in determining the heat transfer from the land surface to the atmosphere. In the SEBS model, the roughness length is estimated using a semi-empirical approach, which can be described as follows:

$$\beta = C_1 - C_2\exp(-C_3C_d \times \mathrm{LAI}) \tag{4}$$

$$n_{ec} = \frac{(C_d \times \mathrm{LAI})}{2\beta^2} \tag{5}$$

$$\frac{d}{h} = 1 - \frac{1}{2n_{ec}}[1 - \exp(-2n_{ec})] \tag{6}$$

$$z_{0m} = h\left[1 - \frac{d}{h}\right]\exp\left(\frac{-k}{\beta}\right) \tag{7}$$

$$h = h_{min} + \frac{h_{max} - h_{min}}{\mathrm{NDVI}_{max} - \mathrm{NDVI}_{min}} \times (\mathrm{NDVI} - \mathrm{NDVI}_{min}) \tag{8}$$

where C_1, C_2, and C_3 are constants linked to the bulk surface drag coefficient, C_d is the leaf drag coefficient, LAI is the leaf area index, n_{ec} is the wind-speed profile extinction coefficient within the canopy, and β is the ratio of the friction velocity to the wind speed at the canopy height. The estimation of canopy height (Equation (8)) follows the equation developed by Chen *et al.* (2013), where h_{min} and h_{max} represent the minimum and maximum canopy heights, respectively, and normalized difference vegetation index $(\mathrm{NDVI})_{max}$ and NDVI_{min} represent the NDVI values of completely vegetated and bare soil, respectively. Roughness length for heat transfer was proposed by Su (2002), as follows:

$$z_{0h} = \frac{z_{0m}}{\exp(kB^{-1})} \tag{9}$$

where kB^{-1} is the inverse Stanton number, which is a scalar heat transfer coefficient.

In the SEBS model, sensible heat (H) and latent heat (LE) fluxes are estimated under limiting cases. LE becomes 0 and H reaches its maximum under dry conditions, while H becomes 0 and LE reaches its maximum under wet conditions. Evaporative fraction (Λ) is then estimated based on these cases, as follows:

$$\Lambda_r = 1 - \frac{H - H_{wet}}{H_{dry} - H_{wet}} \tag{10}$$

$$\Lambda = \frac{LE}{R_N - G} = \frac{\Lambda_r - LE_{wet}}{R_N - G} \tag{11}$$

$$LE = \Lambda \times (R_N - G) \tag{12}$$

where H_{wet} and H_{dry} are H fluxes in wet and dry conditions, and LE_{wet} is the LE in the wet condition. Finally, the instantaneous LE can be estimated by Equation (12).

2.2.2. Input data

The flux tower measures turbulent heat fluxes based on the eddy covariance method and uses them as a ground reference to validate the turbulent heat fluxes estimated by remote-sensing techniques. Flux-tower data were obtained from FLUXNET sites. For SEBS processing, inputs from surface meteorological variables such as pressure, wind speed, air temperature, specific humidity, and shortwave radiation are required, and these variables were measured every half hour.

A total of 15 Landsat 5 Thematic Mapper (TM) images of the 2008–2009 period were downloaded from Global Visualization Viewer USGS (http://glovis.usgs.gov/). Landsat 5 TM, launched in 1984 by NASA, has seven bands, including visible, thermal, and infrared bands. Each band has 30 m spatial resolution, while only band 6 has 120 m spatial resolution and 16 days temporal resolution (https://landsat.usgs.gov/). In this study, a threshold for the cloud cover was set at 10% as a filter to reduce the presence of clouds in the Landsat images. This threshold was to minimize the potential hidden biases in the land surface temperature (LST) result when using optical-based satellite images (Holmes *et al.* 2016; Khand *et al.* 2019). Thus, during the study period, nine images of Landsat 5 were available to be used for the ZM-Mon site and six images were available for the ZA-Kru site. Preprocessing of Landsat images including the conversion of digital numbers to spectral radiance and reflectance was performed, and these conversions were used to derive other inputs, such as albedo, surface emissivity, LAI, NDVI, and LST.

2.3. SPHY model

2.3.1. Methods

Terink *et al.* (2015a) developed the SPHY model, which is a grid-based distributed leaky bucket type of model written in Python language using the dynamical modeling framework of PCRaster. The model has similar soil-column structures to the variable infiltration capacity (VIC) model (Liang *et al.* 1994), including two upper soil storage layers and a groundwater storage layer. SPHY was developed to simulate terrestrial hydrology under various topographical and hydro-climatic conditions, integrating most of the hydrologic processes, and was capable of implementation in a wide range of applications (e.g., climate and land-use change impact, drought, etc.). Other advantages of this model are the lower input data requirement and ability to be forced using remote-sensing data. The differences in spatial resolution from the inputs were addressed by interpolating each dataset to 300 m resolution using bilinear interpolation while maintaining the quality of the data.

The SPHY model used a modified version of the Hargreaves & Samani (1985) equation (Equation (13)) to calculate the reference ET. This equation is efficient for areas with limited meteorological data. The SPHY model calculates the potential ET (ET_p) using the crop coefficient (K_c) approach (Equation (14)), with the crop coefficient value sourced from the literature (Allen *et al.* 1998). Because SPHY is a water balance model, it only considered the pressures associated with water scarcity or plenty when estimating the actual ET (ET_a). The ET reduction parameter ($ETred_{wet}$) utilized by SPHY will take a value of 0 under saturation conditions and a value of 1 under all other conditions. Then, this parameter was used to calculate the ET_a (Equation (15)). For the water shortage condition, the reduction parameter ($ETred_{dry}$) was

calculated using Equation (16):

$$ET_r = 0.0023 \cdot 0.408 \cdot Ra(Tavg + 17.8) \cdot TD^{0.5} \quad (13)$$

$$ET_p = ET_{r,t} \times K_c \quad (14)$$

$$ET_{a,t} = ET_{p,t} \times ETre|d_{wet} \times ETred_{dry} \quad (15)$$

$$ETred_{dry,t} = \frac{SW_{1,t} - SW_{1,pF4.2}}{SW_{1,pF3} - SW_{1,pF4.2}} \quad (16)$$

$$pF = \log_{10}(-H) \quad (17)$$

where Ra is the extraterrestrial radiation (MJ m^{-2} day^{-1}), $ET_{a,t}$ is the actual ET on day t (mm), $ET_{p,t}$ is the potential ET on day t (mm), $ET_{r,t}$ is the reference ET on day t (mm), $ETred_{wet}$ and $ETred_{dry}$ are the reduction parameters for water excess and water shortage conditions, respectively, K_c is the crop coefficient, Tavg is the average daily air temperature (°C), TD is the daily temperature range (°C), pF is the soil water retention parameter, H is the suction force, $SW_{1,t}$ is the soil water content in the first layer of soil at day t (mm), and $SW_{1,pF3}$ and $SW_{1,pF4.2}$ are soil water contents in the first layer at pF3 and pF4 , respectively. In general, soils with a pF of 2 are at field capacity, and soils with a pF of 4.2 are at the permanent wilting point or the point at which the crop dies. Additionally, it was anticipated in SPHY that root water absorption starts to decrease linearly at a pF of 3.

2.3.2. Input data

SPHY required static data and dynamic data as input. The static data were used in this study, which consist of the digital elevation model (DEM), land cover map, and soil characteristics. This model only uses temperature (average, maximal, and minimal) and precipitation as temporal hydro-meteorological data-forcing. In this study, we used daily data over the study period from 2008 to 2009.

2.3.2.1. Precipitation. The Climate Hazards Group InfraRed Precipitation with Station Data (CHIRPS), a 30+ year quasi-global rainfall dataset, was used as the source for the precipitation input. CHIRPS was developed in partnership with researchers at the Earth Resources Observation and Science (EROS) Center of the US Geological Survey (USGS) to provide accurate and comprehensive datasets for early warning purposes (such as trend analysis and seasonal drought monitoring). To construct a gridded rainfall time series for trend analysis, CHIRPS combines *in situ* station data with 0.05° resolution (5 km) satellite imagery starting in 1981 and continuing up to the present.

2.3.2.2. Temperature. The Global Surface Summary of the Day (GSOD) is a gauge-based dataset that includes meteorological data from over 9,000 stations around the world, including mean, maximum, and minimum temperatures. The Integrated Surface Hourly (ISH) database served as the source for GSOD. Inverse distance interpolation has been used to interpolate this station data to 0.1° spatial resolution and the size of the chosen study area.

2.3.2.3. Soil properties. Data on soil hydraulic properties were obtained from the HiHydroSoil map, which was developed by FutureWater. De Boer (2016) showed that the HiHydroSoil map was made by deriving the soil hydraulic parameters from SoilGrids1km. To complete the SoilGrids1km, the Harmonized World Soil Database (HWSD) was used. According to Terink *et al.* (2015a), the SPHY model needed information for the top-soil's saturated water content (mm/mm), field capacity (mm/mm), wilting point (mm/mm), and permanent wilting point (mm/mm), as well as the subsoil layers' saturated water content (mm/mm), field capacity (mm/mm), and saturated conductivity (mm/day).

2.3.2.4. Land cover and DEM. GlobCover, developed by the European Space Agency (ESA), was used as land cover data input in the SPHY model. GlobCover was created using data from the ENVISAT satellite mission's 300 m MERIS sensor (Bicheron *et al.* 2006). In this study, we also used DEM data with 3 arc-sec spatial resolution to derive other parameters such as slope and flow direction maps using the dynamic modeling framework of PCRaster.

2.4. Statistical analysis

We compared both models at the point scale with measured data from two flux-tower sites during specific dates using selected Landsat images. The statistics parameters, consisting of the coefficient of determination (R^2), root-mean-square error (RMSE), average bias, and index of agreement (IOA), were used to evaluate the performance of both models. We also use Taylor's diagram to display the performance of the models.

$$R^2 = \frac{n(\sum E \cdot O) - (\sum E)(\sum O)}{\sqrt{[n\sum E^2 - (\sum E)^2][n\sum O^2 - (\sum O)^2]}} \tag{18}$$

$$\text{bias} = \frac{1}{n}\sum (E - O) \tag{19}$$

$$\text{RMSE} = \sqrt{\frac{1}{n}\sum_{i=1}^{n} (E - O)^2} \tag{20}$$

$$\text{IOA} = 1 - \frac{\sum_{i=1}^{n} (O - E)^2}{\sum_{i=1}^{n} (|E - \bar{O}| + |O - \bar{O}|)^2} \tag{21}$$

where E is the estimation and O is the observation value.

3. RESULTS AND DISCUSSION

3.1. Comparison of ET from SEBS and SPHY with ground-based data

The comparison of estimated ET from the SEBS and SPHY models with measured data using selected dates from Landsat data (Figures 2 and 3) provides valuable insights into the performance of these models. It is evident that the SEBS model tends to overestimate ET, while the SPHY model generally underestimates it. The overestimation by SEBS and underestimation by SPHY can be attributed to the different algorithmic approaches and parameterizations employed by each model and their sensitivity to the input data. Due to the limited available satellite data with low cloud-cover in this study, the comparison of the ET results with ground-based data shows some discrepancies. In future studies, using satellite imagery from multiple sources to increase the number of samples may be an option to reduce the evaluation biases between ET models to the ground observation data and also allow analysis of the annual and long-term ET comparison.

Despite the biases, both models exhibit a reasonable correlation with the measured data. This implies that both SEBS and SPHY capture the underlying processes to some extent, albeit with some discrepancies. Furthermore, when evaluating the performance of the models at specific sites, the SPHY model demonstrates slightly better performance than the SEBS

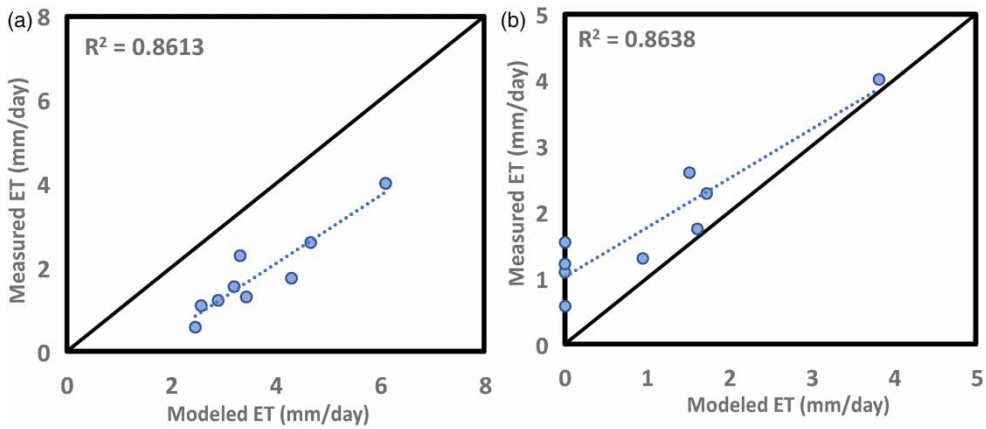

Figure 2 | Comparison of ET from (a) SEBS and (b) SPHY at the Mongu (ZM-Mon) site with *in situ* data.

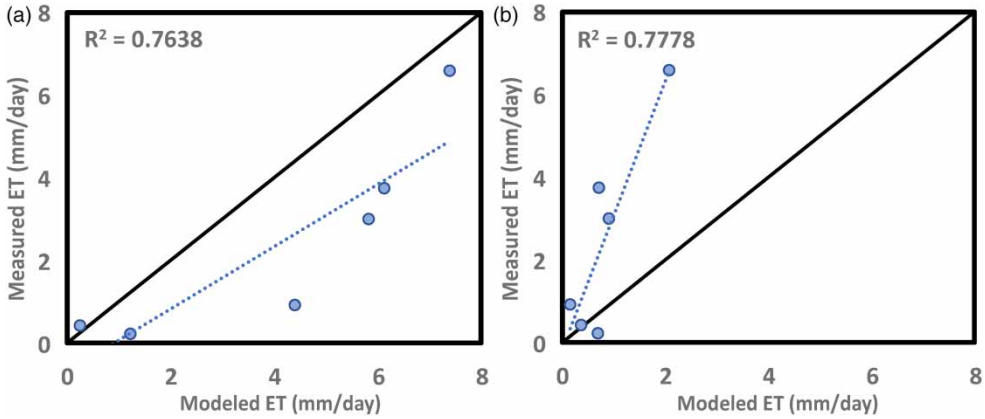

Figure 3 | Comparison of ET from (a) SEBS and (b) SPHY at the Skukuza (ZM-Kru) site with *in situ* data.

model. The coefficients of determination (R^2 value) of 0.86 for SPHY at the Mongu site and 0.78 at the Skukuza site indicate a relatively strong relationship between the estimated and measured ET values. These values suggest that the SPHY model explains approximately 86% and 78% of the variability in ET at the Mongu and Skukuza sites, respectively. The analysis of Figures 2 and 3 highlights the contrasting tendencies of the SEBS and SPHY models to overestimate and underestimate ET, respectively. The SPHY model demonstrates slightly better performance at the specific sites analyzed, as indicated by the higher coefficient of determination.

3.2. Effect of hydrological variables on daily ET

The analysis of ET results using the SPHY model reveals its sensitivity to the main forcing data, particularly precipitation (Figures 4 and 5). It is observed that during the summer season, characterized by high rates of precipitation, the SPHY model tends to overestimate ET for both sites. Conversely, in periods of low precipitation, the model underestimates ET, particularly at the ZM-Mon site (forest) (Figure 4). The analysis of the SPHY model's sensitivity to precipitation and its impact on

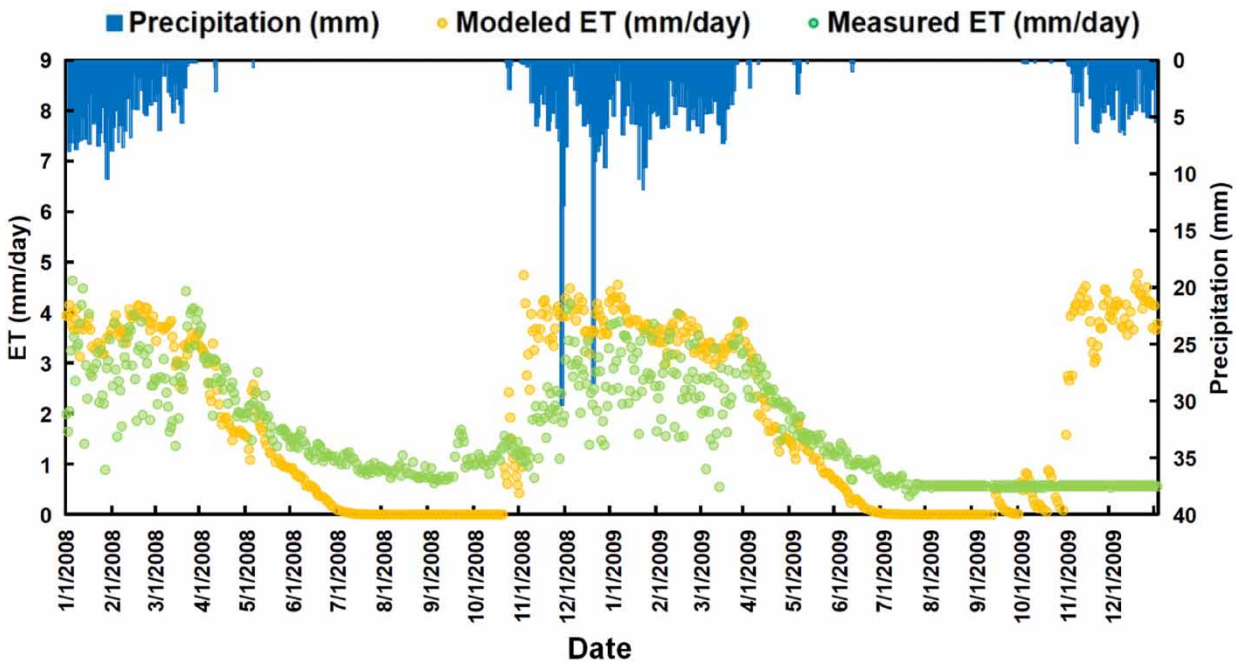

Figure 4 | Effect of precipitation variable on daily SPHY simulated ET for the study period 2008–2009 at the Mongu (ZM-Mon) site.

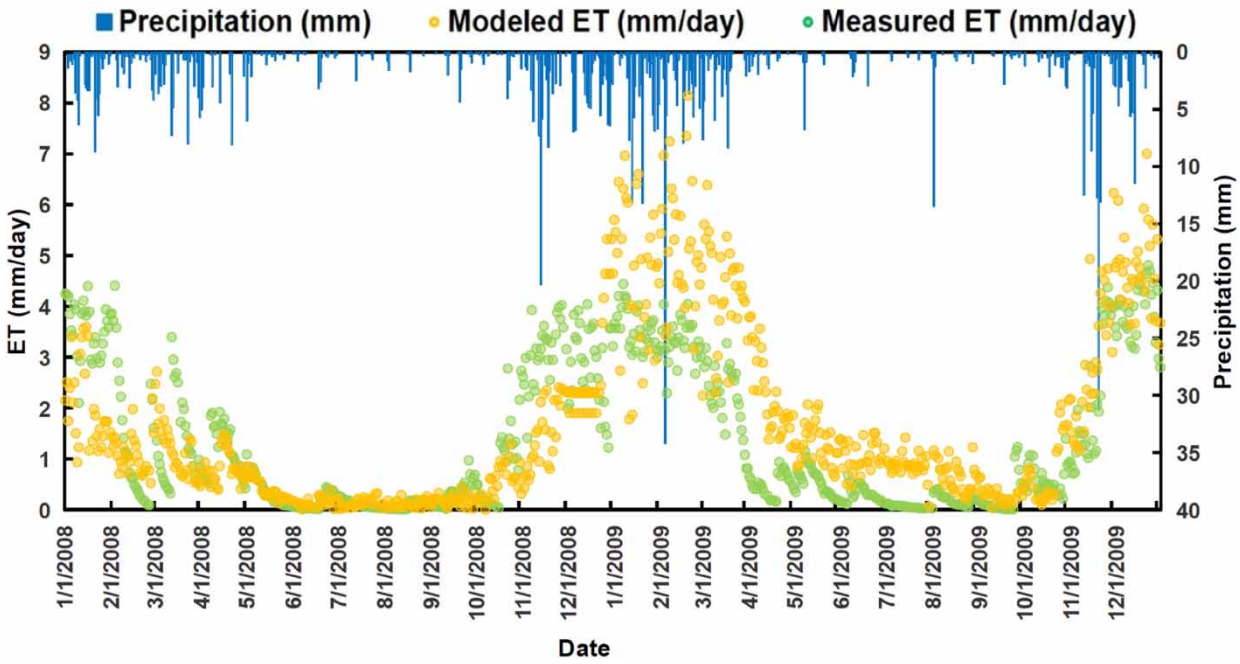

Figure 5 | Effect of precipitation variable on daily SPHY simulated ET for the study period 2008–2009 at the Skukuza (ZM-Kru) site.

ET aligns with previous studies. The findings that the SPHY model tends to overestimate ET during high precipitation periods and underestimate it during low precipitation periods are consistent with those of studies such as Bližňák *et al.* (2022). These studies highlight the importance of considering the temporal variability and intensity of precipitation in ET models and acknowledge the potential biases that can arise from the improper representation of precipitation dynamics.

The SPHY model relies heavily on precipitation and temperature as the primary dynamic input data for calculating ET, utilizing water content variables from the current day and the previous day (Equation (16)). This dependency on precipitation and temperature can explain the overestimation during the summer season and the underestimation during the winter season, which might be influenced by the dependency of the SPHY model on water excess and water shortage stress parameters to calculate the actual ET (Terink *et al.* 2015c). In the summer, the model may overestimate ET due to high precipitation rates, which could result in the calculation of higher ET values. Conversely, during periods of low precipitation in the winter, the model may underestimate ET since there is less water available for ET. The dependency of the SPHY model on precipitation and temperature as the main dynamic input data for ET calculation is in line with the broader literature on ET modeling. For instance, Zhang *et al.* (2019) emphasized the significance of incorporating accurate precipitation and temperature data to improve ET estimation, as these variables strongly drive the availability of water for ET processes. The observation that zero precipitation and low water content lead to zero ET values and increased drought intensity aligns with the concept of water limitation on ET, as discussed by Teuling *et al.* (2013). These authors highlighted that drought conditions can severely restrict the availability of water for ET, resulting in reduced or even negligible ET rates.

In the middle of the winter season, the estimated ET values reach zero due to the combined effects of zero precipitation and low water content, leading to an increase in drought intensity. The SPHY model captures this phenomenon, as the lack of precipitation and minimal water content result in limited ET. At the ZM-Kru (savanna) site, the model only slightly underestimates ET due to temporal precipitation, even in small quantities (Figure 5).

3.3. Sensitivity analysis of SPHY and SEBS on different land covers

Both models showed a good correlation with measured data from the flux tower, indicating their ability to capture the underlying processes. Overall, the two models showed better performance at the ZM-Mon site and marginal performance at the ZM-Kru site, perhaps because of the slightly higher elevation and more homogeneous vegetation at the ZM-Mon site, where woody vegetation predominates with around 60% coverage (based on the information from https://fluxnet.org),

compared with the ZM-Kru site (savanna) characterized by vegetation heterogeneity, including various herbaceous and forest-canopy types covering around 10%–30%. This pattern of the ET model is in agreement with the result discussed in Liaqat & Choi (2015).

When comparing the RMSE between the two models, it was observed that the SEBS model exhibited a slightly lower RMSE (2.17 mm day^{-1}) at the ZM-Kru site, which is a savanna ecosystem, than the SPHY model (2.27 mm day^{-1}) (Table 2). These differences might be attributed to the SEBS model's ability to better depict ET in the heterogeneity of the savanna ecosystem due to the more detailed energy balance components in the SEBS than in the SPHY model, which used a water balance system in its algorithm. On the other hand, the SPHY model showed a lower RMSE (0.88 mm day^{-1}) than the SEBS model (1.90 mm day^{-1}) at the ZM-Mon site, representing a forest ecosystem with most of the land covered by woody vegetation. In the SPHY algorithm, the calculation of ET used an evaporation reduction parameter influenced by the soil saturation value instead of using detailed plant and soil properties as input to the model. Thus, the SPHY model can calculate reasonable ET at a site with more homogeneous vegetation than a site with heterogeneous vegetation types. These findings suggest that the performance of the two models varies depending on the ecosystem type. The SPHY model exhibited a reasonable performance compared with the SEBS model at the ZM-Mon site (forest), while the SEBS model performed slightly better at the ZM-Kru site (savanna). It is important to note that both models yielded high IOA values for both sites, indicating that they generally reproduced the observed data well.

Additionally, the bias analysis revealed interesting insights. The positive bias observed for the SEBS model indicates an overestimation of the fluxes compared with the measured data, whereas the negative bias for the SPHY model suggests an underestimation (Figure 6). This implies that the SEBS model tends to overestimate the fluxes, while the SPHY model tends to underestimate them. Considering the overall performance of the two models across both sites, it can be concluded that the SPHY model performed better than the SEBS model. However, it is worth noting that the performance comparison may vary in different ecosystems and under different conditions. The sensitivity of the SPHY model to precipitation and temperature as the main driving forces for ET calculation leads to its performance variations in different seasons and ecosystems. The model's tendency to overestimate ET during summer and underestimate it during low precipitation periods in winter highlights the importance of accurately representing these inputs for improved ET estimation. Further analysis and evaluation are required to fully understand the strengths and limitations of each model in various settings.

4. CONCLUSION

This study aimed to compare the estimation of ET using two different framework models: the energy-based model (SEBS) and the water balance model (SPHY). The results were compared with ground observation data from the flux towers of FLUXNET sites (ZM-Mon and ZM-Kru), which are located in different PFT types across southeast Africa. The results demonstrate that both models exhibit a good correlation with the measured data from flux towers with R^2 (RMSE) values ranging from 0.76 to 0.86 (0.88 to 2.27 mm day^{-1}), indicating their ability to capture the underlying processes of ET. The performance of the SPHY model generally produced reasonable results compared with the SEBS model. Both models have their advantages and limitations in different land cover types. The SPHY model demonstrates a lower RMSE in forest areas with homogeneous vegetation, suggesting its reasonable performance in capturing ET dynamics in such ecosystems. On the other hand, the SEBS model shows slightly better performance in savanna areas, as indicated by lower RMSE values, than the SPHY model. These findings emphasize the importance of considering the specific characteristics of different land cover types, including the vegetation composition, when interpreting the results of ET models.

Table 2 | Statistical parameters for discrepancies between SEBS and SPHY models with *in situ* reference data

Model	Site	R^2	RMSE	BIAS	IOA
SEBS	ZM-Mon	0.86	1.90	1.84	0.60
	ZM-Kru	0.76	2.17	1.81	0.81
SPHY	ZM-Mon	0.86	0.88	−0.75	0.85
	ZM-Kru	0.78	2.27	−1.48	0.58

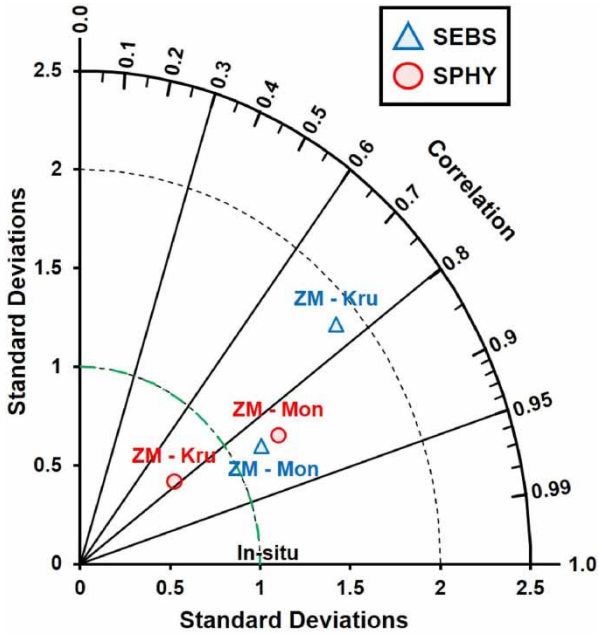

Figure 6 | Taylor's diagram for ET estimates using SEBS and SPHY models for Mongu (ZM-Mon; forest) and Skukuza (ZM-Kru; savanna) sites.

The sensitivity analysis reveals that the SPHY model is significantly influenced by the rate of precipitation as input data. During summer seasons with high precipitation rates, the model tends to overestimate ET, while in low precipitation periods, it underestimates ET, especially at the ZM-Mon site with forest ecosystems. These findings highlight the need for the accurate representation of precipitation dynamics in ET models to improve their performance. Furthermore, both models display seasonal variations in ET estimation, with overestimation in the wet period and underestimation in the dry period. The occurrence of near-zero ET values during periods of intense drought further emphasizes the sensitivity of the models to water availability.

To enhance the accuracy of estimated actual ET, future studies should focus on conducting uncertainty analyses for the input data of each model, especially precipitation data that majorly influence the ET result. Exploring uncertainties associated with various input variables can provide insights into the reliability and limitations of the estimated ET values. Improving the spatial resolution of input data is crucial as it can impact the model's output and enhance the representation of spatial heterogeneity in ET estimation. Additionally, using more satellite data from multiple sources in future studies can be an option to increase the number of samples to provide analysis for the long-term period and reduce biases due to the limited cloud-free satellite imagery available. This work is expected to benefit other studies that develop machine-learning paradigms in selecting data usage for ET prediction by evaluating the influence of the amount of input data and model efficiency correlates.

DATA AVAILABILITY STATEMENT

All relevant data are included in the paper or its Supplementary Information.

CONFLICT OF INTEREST

The authors declare there is no conflict.

REFERENCES

Allen, R. G., Pereira, L. S., Raes, D. & Smith, M. 1998 *Crop Evapotranspiration – Guidelines for Computing Crop Water Requirements*. FAO Irrigation and Drainage Paper 56, Food and Agriculture Organization of the United Nations, Rome, Italy. Available from: https://www.researchgate.net/publication/235704197.

Bicheron, P., Leroy, M., Brockmann, C., Krämer, U., Miras, B., Huc, M., Ninõ, F., Defourny, P., Vancutsem, C., Arino, O., Ranéra, F., Petit, D., Amberg, V., Berthelot, B. & Gross, D. 2006 GLOBCOVER: a 300m global land cover product for 2005 using ENVISAT MERIS time series. In: *ISPRS Commission VII Symposium: Remote Sensing from Pixels to Processes*, 8–11 May, Enschede, The Netherlands. Available from: https://www.researchgate.net/publication/285769150.

Bližňák, V., Pokorná, L. & Rulfová, Z. 2022 Assessment of the capability of modern reanalyses to simulate precipitation in warm months using adjusted radar precipitation. *Journal of Hydrology: Regional Studies* **42**, 101121. https://doi.org/10.1016/j.ejrh.2022.101121.

Brutsaert, W. 1982 *Evaporation into the Atmosphere: Theory, History, and Applications*. Springer, Dordrecht, The Netherlands.

Byun, K., Liaqat, U. W. & Choi, M. 2014 Dual-model approaches for evapotranspiration analyses over homo- and heterogeneous land surface conditions. *Agricultural and Forest Meteorology* **197**, 169–187. https://doi.org/10.1016/J.AGRFORMET.2014.07.001.

Chen, X., Su, Z., Ma, Y., Yang, K., Wen, J. & Zhang, Y. 2013 An improvement of roughness height parameterization of the Surface Energy Balance System (SEBS) over the Tibetan plateau. *Journal of Applied Meteorology and Climatology* **52** (3), 607–622. https://doi.org/10.1175/JAMC-D-12-056.1.

De Boer, F. 2016 *HiHydroSoil: A High Resolution Soil Map of Hydraulic Properties, Version 1.2*. FutureWater Report 134, FutureWater, Wageningen, The Netherlands. Available from: www.futurewater.nl.

Eekhout, J. P. C., Terink, W. & de Vente, J. 2018 Assessing the large-scale impacts of environmental change using a coupled hydrology and soil erosion model. *Earth Surface Dynamics* **6** (3), 687–703. https://doi.org/10.5194/esurf-6-687-2018.

Ershadi, A., McCabe, M. F., Evans, J. P., Chaney, N. W. & Wood, E. F. 2014 Multi-site evaluation of terrestrial evaporation models using FLUXNET data. *Agricultural and Forest Meteorology* **187**, 46–61. https://doi.org/10.1016/J.AGRFORMET.2013.11.008.

Fisher, J. B., Tu, K. P. & Baldocchi, D. D. 2008 Global estimates of the land–atmosphere water flux based on monthly AVHRR and ISLSCP-II data, validated at 16 FLUXNET sites. *Remote Sensing of Environment* **112** (3), 901–919. https://doi.org/10.1016/j.rse.2007.06.025.

Gokmen, M., Vekerdy, Z., Verhoef, A., Verhoef, W., Batelaan, O. & van der Tol, C. 2012 Integration of soil moisture in SEBS for improving evapotranspiration estimation under water stress conditions. *Remote Sensing of Environment* **121**, 261–274. https://doi.org/10.1016/J.RSE.2012.02.003.

Hargreaves, G. H. & Samani, Z. A. 1985 Reference crop evapotranspiration from temperature. *Applied Engineering in Agriculture* **1** (2), 96–99. https://doi.org/10.13031/2013.26773.

Holmes, T. R. H., Hain, C. R., Anderson, M. C. & Crow, W. T. 2016 Cloud tolerance of remote-sensing technologies to measure land surface temperature. *Hydrology and Earth System Sciences* **20** (8), 3263–3275. https://doi.org/10.5194/hess-20-3263-2016.

Hwang, K. & Choi, M. 2013 Seasonal trends of satellite-based evapotranspiration algorithms over a complex ecosystem in East Asia. *Remote Sensing of Environment* **137**, 244–263. https://doi.org/10.1016/J.RSE.2013.06.006.

Khand, K., Taghvaeian, S., Gowda, P. & Paul, G. 2019 A modeling framework for deriving daily time series of evapotranspiration maps using a surface energy balance model. *Remote Sensing* **11** (5), 508. https://doi.org/10.3390/rs11050508.

Liang, X., Lettenmaier, D. P., Wood, E. F. & Burges, S. J. 1994 A simple hydrologically based model of land surface water and energy fluxes for general circulation models. *Journal of Geophysical Research Atmospheres* **99** (D7), 14415–14428. https://doi.org/10.1029/94jd00483.

Liaqat, U. W. & Choi, M. 2015 Surface energy fluxes in the Northeast Asia ecosystem: SEBS and METRIC models using Landsat satellite images. *Agricultural and Forest Meteorology* **214–215**, 60–79. https://doi.org/10.1016/j.agrformet.2015.08.245.

Liaqat, U. W., Choi, M. & Awan, U. K. 2015 Spatio-temporal distribution of actual evapotranspiration in the Indus Basin Irrigation System. *Hydrological Processes* **29** (11), 2613–2627. https://doi.org/10.1002/hyp.10401.

Long, D., Longuevergne, L. & Scanlon, B. R. 2014 Uncertainty in evapotranspiration from land surface modeling, remote sensing, and GRACE satellites. *Water Resources Research* **50** (2), 1131–1151. https://doi.org/10.1002/2013WR014581.

Lu, J., Li, Z. L., Tang, R., Tang, B. H., Wu, H., Yang, F., Labed, J. & Zhou, G. 2013 Evaluating the SEBS-estimated evaporative fraction from MODIS data for a complex underlying surface. *Hydrological Processes* **27** (22), 3139–3149. https://doi.org/10.1002/hyp.9440.

Ma, W., Hafeez, M., Rabbani, U., Ishikawa, H. & Ma, Y. 2012 Retrieved actual ET using SEBS model from Landsat-5 TM data for irrigation area of Australia. *Atmospheric Environment* **59**, 408–414. https://doi.org/10.1016/J.ATMOSENV.2012.05.040.

Queface, A. J., Piketh, S. J., Eck, T. F., Tsay, S. C. & Mavume, A. F. 2011 Climatology of aerosol optical properties in Southern Africa. *Atmospheric Environment* **45** (17), 2910–2921. https://doi.org/10.1016/J.ATMOSENV.2011.01.056.

Senay, G. B., Budde, M. E. & Verdin, J. P. 2011 Enhancing the Simplified Surface Energy Balance (SSEB) approach for estimating landscape ET: validation with the METRIC model. *Agricultural Water Management* **98** (4), 606–618. https://doi.org/10.1016/J.AGWAT.2010.10.014.

Su, Z. 2002 The Surface Energy Balance System (SEBS) for estimation of turbulent heat fluxes. *Hydrology and Earth System Sciences* **6** (1), 85–100. https://doi.org/10.5194/hess-6-85-2002.

Terink, W., Lutz, A. F. & Immerzeel, W. W. 2015a *SPHY: Spatial Processes in Hydrology. Graphical User-Interfaces (GUIs)*. FutureWater Report 143, FutureWater, Wageningen, The Netherlands. Available from: http://www.adb.org/.

Terink, W., Lutz, A. F. & Immerzeel, W. W. 2015b *SPHY v2.0: Spatial Processes in Hydrology. Model Theory, Installation, and Data Preparation*. FutureWater Report 142, FutureWater, Wageningen, The Netherlands.

Terink, W., Lutz, A. F., Simons, G. W. H., Immerzeel, W. W. & Droogers, P. 2015c SPHY v2.0: Spatial Processes in HYdrology. *Geoscientific Model Development* **8** (7), 2009–2034. https://doi.org/10.5194/gmd-8-2009-2015.

Teuling, A. J., Van Loon, A. F., Seneviratne, S. I., Lehner, I., Aubinet, M., Heinesch, B., Bernhofer, C., Grünwald, T., Prasse, H. & Spank, U. 2013 Evapotranspiration amplifies European summer drought. *Geophysical Research Letters* **40** (10), 2071–2075. https://doi.org/10.1002/grl.50495.

Zhang, H., Wu, C., Chen, W. & Huang, G. 2019 Effect of urban expansion on summer rainfall in the Pearl River Delta, South China. *Journal of Hydrology* **568**, 747–757. https://doi.org/10.1016/j.jhydrol.2018.11.036.

First received 27 August 2023; accepted in revised form 13 January 2024. Available online 30 January 2024